Supporting Information

Molecular Shape Recognition by Using a Switchable Luminescent Nonporous Molecular Crystal

Hiroaki Imoto[†], Susumu Tanaka[†], Takuji Kato[†], Takashi Yumura[‡], Seiji Watase[§], Kimihiro Matsukawa[†§], and Kensuke Naka*[,†]

[†] Faculty of Molecular Chemistry and Engineering, Graduate School of Science and Technology, Kyoto Institute of Technology, Goshokaido-cho, Matsugasaki, Sakyo-ku, Kyoto 606-8585, Japan.

[‡] Faculty of Materials Science and Engineering, Graduate School of Science and Technology, Kyoto Institute of Technology, Goshokaido-cho, Matsugasaki, Sakyo-ku, Kyoto 606-8585, Japan.

[§] Osaka Municipal Technical Research Institute, 1-6-50 Morinomiya, Joto-ku, Osaka 536-8553, Japan.

Contents:

1. Materials

Chlorobenzene (PhCl), toluene, *n*-hexane, cyclohexane, dichloromethane (CH_2Cl_2), chloroform ($CHCl_3$), tetrahydrofuran (THF), 1,4-dioxane, methanol (MeOH), ethanol (EtOH), 2-propanol (*i*PrOH), and acetonitrile (MeCN) were purchased from Nacalai Tesque, Inc. 1-Pentanol, diethyl ether (Et_2O) and benzene were purchased from Wako Pure Chemical Industry, Ltd. All commercially available chemicals were used without further purification. Platinum dibromide complex with 9-phenyl-9-arsafluorene (**1**) was prepared by following the literature.[1]

2. Measurement

^1H (400 MHz) NMR spectra were recorded on a Bruker DPX-400 spectrometers, and samples were analyzed in $CDCl_3$ using Me_4Si as an internal standard. Emission spectra were obtained on a JASCO fluorescence spectrophotometer FP-8500, and absolute PL quantum yields (Φ) were determined using a JASCO ILFC-847S. X-ray diffractions (XRD) were recorded on a Rigaku RAXIS RAPID II imaging plate area detector using monochromated Cu Kα radiation by rotating samples along the φ-axis and transformed to 2θ-I plot by software.

3. X-ray crystallographic data for single crystalline products

The single crystal was mounted on glass fibers with epoxy resin. Intensity data were collected at room temperature on a Rigaku RAXIS RAPID II imaging plate area detector with graphite monochromated Mo Kα radiation. The crystal-to-detector distance was 127.40 mm. Readout was performed in the 0.100 mm pixel mode. The data were collected at room temperature to a maxim m 2θ value of 55.0°. Data were processed by the PROCESS-AUTO[2] program package. An empirical or numerical absorption correction[3] was applied. The data were corrected for Lorentz and polarization effects. A correction for secondary extinction[4] was applied. The structure was solved by heavy atom Patterson methods[5] and expanded using Fourier techniques.[6] Some non-hydrogen atoms were refined anisotropically, while the rest were refined isotropically. Hydrogen atoms were refined using the riding model. The final cycle of full-matrix least-squares refinement on F^2 was based on observed reflections and variable parameters. In the case of the crystalline product recrystallized from acetone, the final cycle of full-matrix least-squares refinement on F was based on observed reflections and variable parameters. All calculations were performed using the

CrystalStructure[7,8] crystallographic software package. Crystal data and more information on X-ray data collection are summarized in Tables S1-S3.

4. Sample preparation

4-1. Recrystallization

1·PhCl and **1**·CH_2Cl_2 were prepared by recrystallization. A PhCl solution of **1** was heated at 130°C, and subsequently the solution was slowly cooled to room temperature to obtain **1**·PhCl. On the other hand, **1**·CH_2Cl_2 was prepared by slow mixing of MeOH to the CH_2Cl_2 solutions.

4-2. Exposure to VOCs

1·PhCl (3 mg) was put in a 5 mL sample tube. The sample tube was put in a 10 mL sample tube, and subsequently liquid of a VOC was poured into the 10 mL sample tube (Figure S1). During the experiment, the ambient temperature was kept at 25 °C.

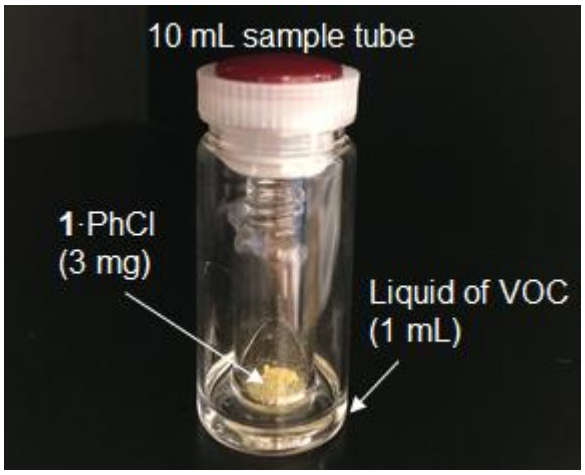

Figure S1. Photograph of vapor fuming experiment.

5. Crystallographic data

Table S1. Crystallographic Data.

	1·PhCl	**1**·CH_2Cl_2[1]
Crystal data		
Empirical Formula	C42H31As2Br2ClPt	C36.5H27As2Br2ClPt
Formula Weight	1075.90	1005.81
Crystal Dimension, mm^3	0.200 × 0.100 × 0.100	0.200 × 0.150 × 0.150
Crystal System	triclinic	triclinic
Space Group	P-1	P-1
a, Å	9.0753(3)	8.9649(2)
b, Å	9.9531(3)	9.8619(3)
c, Å	10.7614(3)	19.2946(6)
α, deg	100.7631(7)	96.9662(14)
β, deg	94.6827(10)	100.3116(12)
γ, deg	100.0884(10)	97.5634(11)
Volume, $Å^3$	933.58(5)	1645.25(9)
D_{calcd}, g cm^{-3}	1.914	2.030
Z	1	2
F(000)	514.00	954.00
Data Collection		
Temperature, deg	23.0	23.0
2θmax, deg	54.9	54.9
Tmin/Tmax	0.162 / 0.461	0.165 / 0.268
Refinement		
No. of Observed Data	4238	7490
No. of Parameters	215	372
R1[a], wR2[b]	0.0400, 0.1181	0.0347, 0.1105
Goodness of Fit Indictor	1.139	1.084

[a]$R1 = \Sigma \, | \, |Fo| - |Fc| \, | \, / \, \Sigma \, |Fo|$ [b]$wR2 = [\, \Sigma \, w \, ((Fo^2-Fc^2)^2 \, / \, \Sigma \, w \, (Fo^2)^2 \,]^{1/2}$ $w = [\, \sigma^2(Fo^2) \,]^{-1}$

CCDC # 1455870 (**1**·PhCl) and 1419056 (**1**·CH_2Cl_2)

Table S2. ORTEP drawing (ellipsoids at 50% probability), selected angles (deg), and distance (Å) of **1**·PhCl.

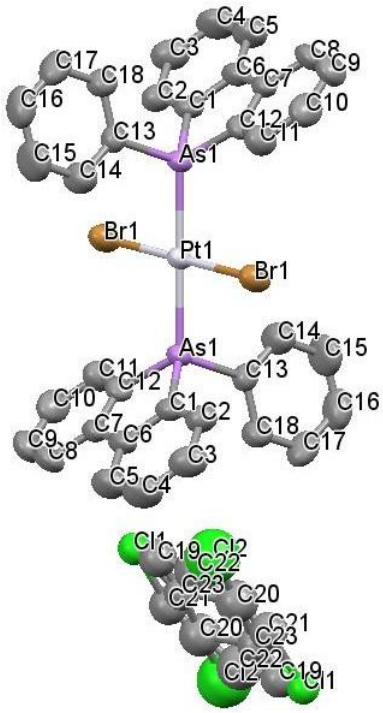

distances (Å)		angles (°)	
Pt(1)-Br(1)	2.4275(6)	As(1)-Pt(1)-Br(1)	93.52(2)
			86.48(2)
Pt(1)-As(1)	2.3987(6)	Br(1)-Pt(1)-Br(1)	180.00(3)
As(1)-C(1)	1.929(6)	C(1)-As(1)-C(12)	88.7(3)
As(1)-C(12)	1.925(5)	C(1)-As(1)-C(13)	105.4(2)
As(1)-C(13)	1.933(7)	C(12)-As(1)-C(13)	105.4(3)

Table S3. ORTEP drawing (ellipsoids at 50% probability), selected angles (deg), and distance (Å) of **1**·CH_2Cl_2.[1]

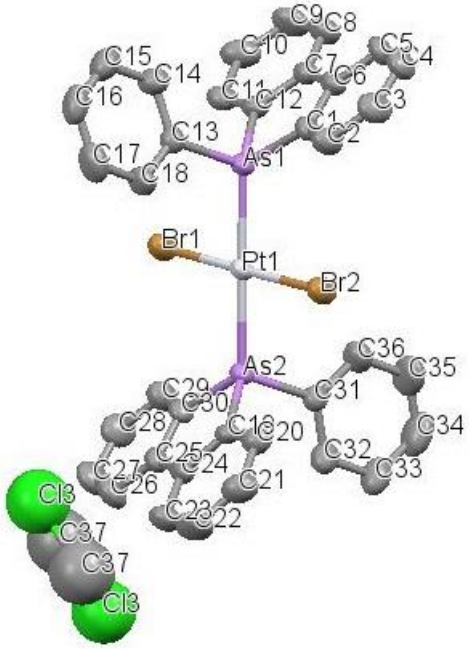

distances (Å)	
Pt(1)-Br(1)	2.4229(8)
Pt(1)-Br(2)	2.4335(8)
Pt(1)-As(1)	2.3952(8)
Pt(1)-As(2)	2.3954(8)
As(1)-C(1)	1.918(6)
As(1)-C(12)	1.929(7)
As(1)-C(13)	1.923(8)
As(2)-C(19)	1.938(7)
As(2)-C(30)	1.926(6)
As(2)-C(31)	1.932(8)

angles (°)	
As(1)-Pt(1)-Br(1)	86.25(3)
As(1)-Pt(1)-Br(2)	93.09(3)
As(2)-Pt(1)-Br(1)	93.39(3)
As(2)-Pt(1)-Br(2)	87.28(3)
Br(1)-Pt(1)-Br(2)	179.16(3)
As(1)-Pt(1)-As(2)	179.00(3)
C(1)-As(1)-C(12)	88.4(3)
C(1)-As(1)-C(13)	104.2(3)
C(12)-As(1)-C(13)	106.8(3)
C(19)-As(2)-C(30)	88.2(3)
C(19)-As(2)-C(30)	104.4(3)
C(30)-As(2)-C(31)	103.8(3)

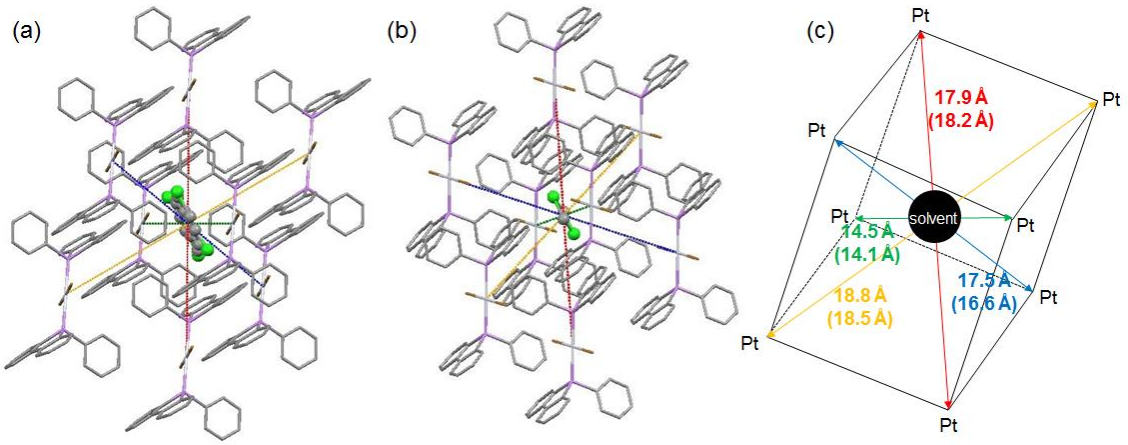

Figure S2. Packing structure of (a) **1**·PhCl and (b) **1**·CH_2Cl_2 based on the single crystal X-ray diffraction. (c) Intermolecular Pt–Pt distances of **1**·PhCl (bare) and **1**·CH_2Cl_2 (bracket).

6. Optical properties

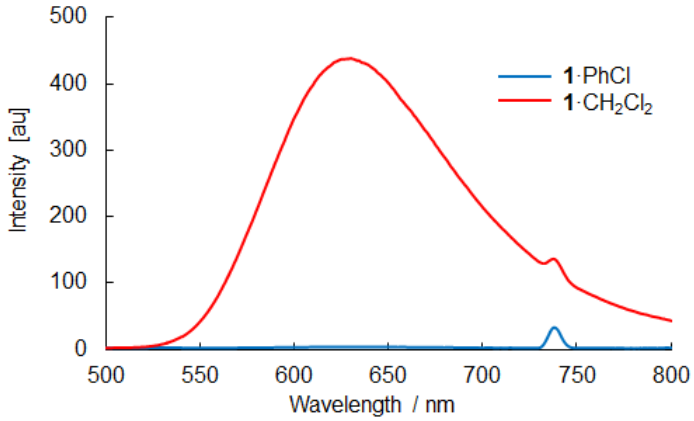

Figure S3. Solid-state photoluminescence spectra of **1**·PhCl and **1**·CH_2Cl_2 (excited at 370 nm).

7. Theoretical calculation

(i) Single-point energy DFT calculations with B3LYP functional were performed by using the **1**…PhCl geometries obtained from the crystallographic studies (Figure S4(a)). During the DFT calculations implemented in the Gaussian 09 code[9] we used the CEP-121G basis set for the Pt atom, and the 6-311G* basis set for the As, Br, C, Cl, and H atoms. DFT calculations found substantial orbital overlaps between the **1** complex and chlorobenzene in the HOMO-6 and LUMO+4 (Figure S4(b)), which can assist electron transfers between the two.

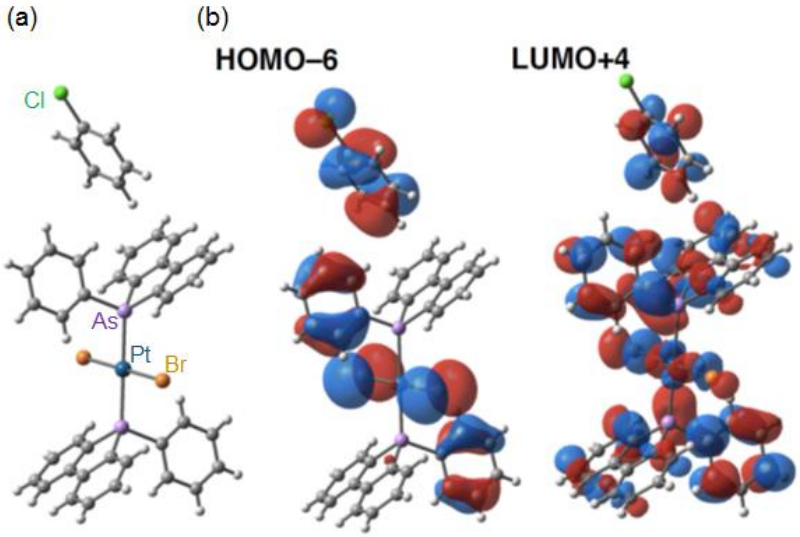

Figure S4. (a) Geometry of **1**·PhCl based on the single crystal X-ray diffraction. (b) Examples of B3LYP-calculated molecular orbitals exhibiting the overlaps between **1** and PhCl. The calculation was carried out in Gaussian 09.

(ii) To gain information on the energetics of the **1** crystals immersed by PhCl or CH_2Cl_2 from the crystallographic studies, periodic boundary condition (PBC) DFT calculations with PBE functional were performed. Then, projector augmented plane wave (PAW) pseudopotential and kinetic energy cut-off of plane wave of 400 eV were used in the VASP code. A 4 × 4 × 4 *k*-point mesh was used for the single-point calculations, because we confirmed the total energy is converged with this k-point mesh. By using the PBE calculations, we estimated the total energy of the **1** crystals obtained from the crystallographic studies by removing PhCl or CH_2Cl_2 solvents. The PBE calculations found that the **1** crystal obtained by removing PhCl is only 1.1 kcal/mol stable relative to that by removing CH_2Cl_2, indicating that there is no significant difference in the conformational stability between **1**·PhCl and **1**·CH_2Cl_2.

8. NMR study

The filling degrees of the crystals were estimated by ^{1}H NMR spectra in CD_2Cl_2 (Figure S5). The filling degrees of **1**·PhCl and **1**·PhCl(soak) were 74% and 73%, respectively. On the other hand, that of **1**·CH_2Cl_2(vap) was less than 1%.

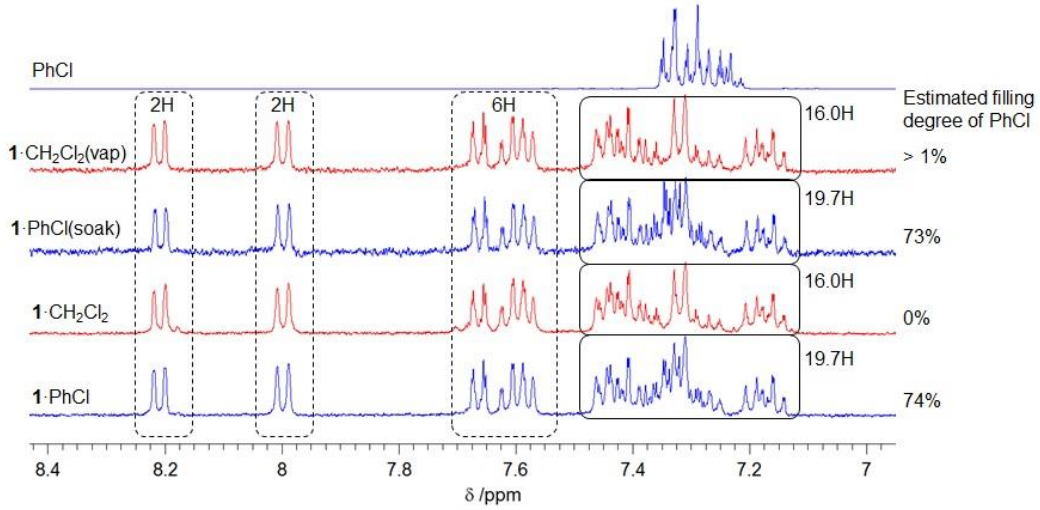

Figure S5. ^{1}H NMR spectra (400 MHz, in CD_2Cl_2) of **1**·PhCl, **1**·CH_2Cl_2, **1**·PhCl(soak), **1**·CH_2Cl_2(vap), and PhCl.

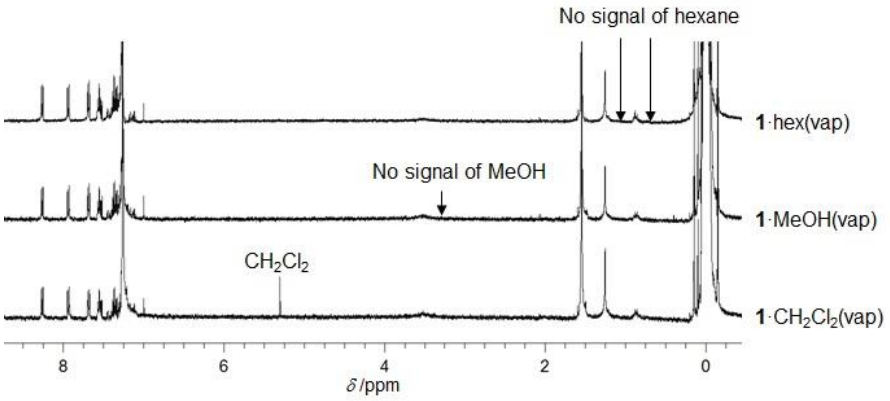

Figure S6. ^{1}H NMR spectra (400 MHz, in $CDCl_3$) of **1**·CH_2Cl_2(vap), **1**·MeOH(vap), and **1**·hex(vap).

9. XRD patterns

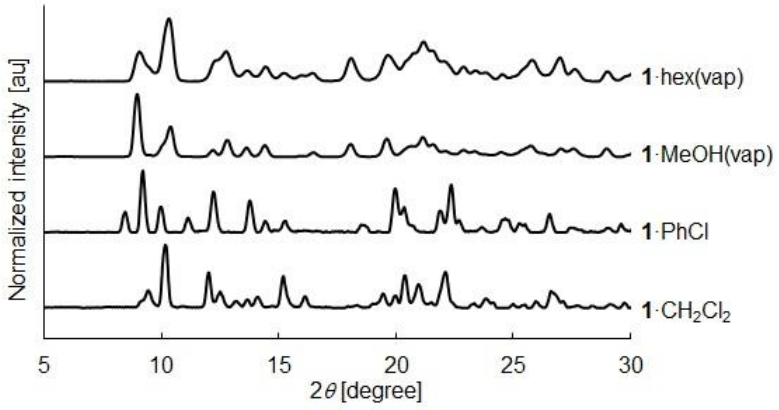

Figure S7. XRD patterns of **1**·MeOH(vap), and **1**·hex(vap), **1**·CH_2Cl_2, and **1**·PhCl.

10. Thermal analyses

The TGA thermogram of **1**·PhCl suggests that 67-78% of the cavities in the crystal matrix were filled by PhCl molecules. The DSC curves of the first cycle shows a clear endothermic signal around 120-155 °C, while the signal disappears in the second cycle. Therefore, the signal around 120-155 °C is derived from the evaporation of the encapsulated PhCl molecules.

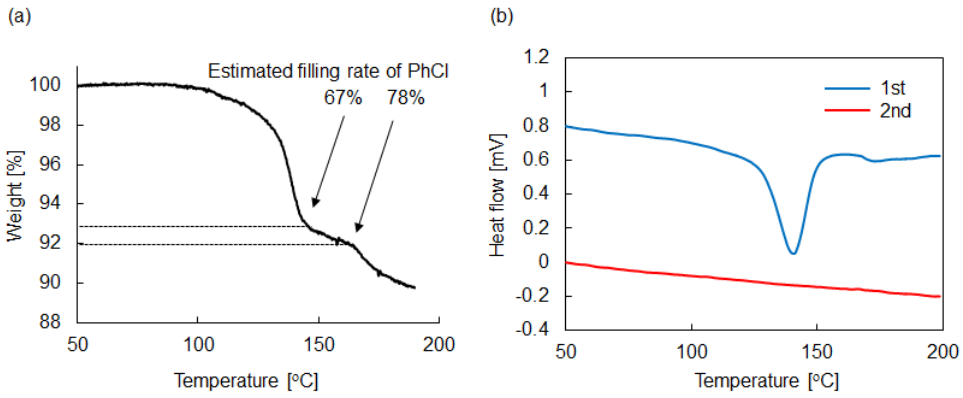

Figure S8. (a) TGA thermogram and (b) DSC curves of **1**·PhCl (under N_2, 10 °C/min).

11. VOC sensing

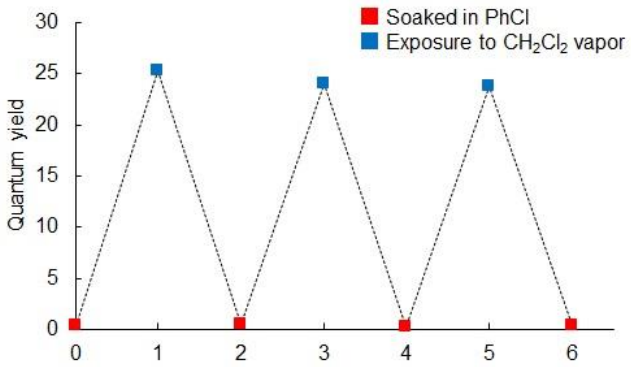

Figure S9. Quantum yields during the cycle of soaking in PhCl (36 h) and exposure to CH_2Cl_2 vapor (36 h).

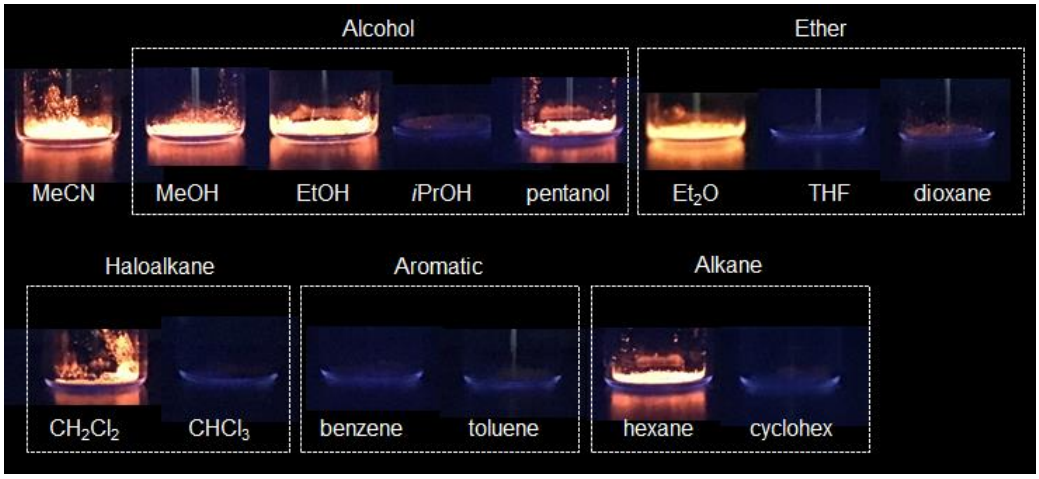

Figure S10. Photographs of the samples after the exposure to VOC vapors for 36 h (under irradiation at 365 nm).

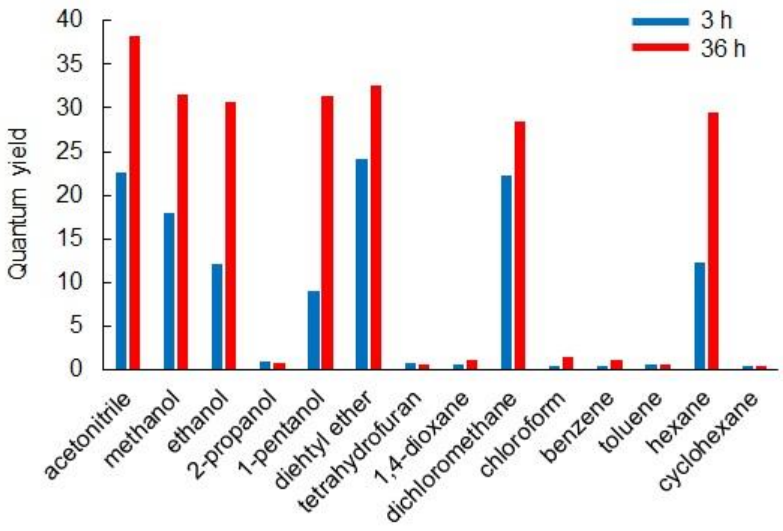

Figure S11. Quantum yields after exposure to various VOCs for 3 h and 36 h.

12. References

[1] H. Imoto, S. Tanaka, T. Kato, S. Watase, K. Matsukawa, T. Yumura and K. Naka, *Organometallics* **2016**, *35*, 364.

[2] *PROCESS-AUTO, RAXIS data-processing software;* Rigaku Corporation: Tokyo, Japan, 1996.

[3] T. Higashi, *FS_ABSCOR, Program for Absorption Correction;* Rigaku Corporation: Tokyo, Japan, 1995.

[4] A. C. Larson, *Crystallographic Computing;* F. R. Ahmed, Ed.; Munksgaard: Copenhagen, Denmark, **1970**, 291−294.

[5] P. T. Beurskens, G. Admiraal, G. Beurskens, W. P. Bosman, R. de Gelder, R. Israel, J. M. M. Smits, *The DIRDIF-99 Program System;* Technical Report of the Crystallography Laboratory, University of Nijmegen: Nijmegen, The Netherlands, 1999.

[6] P. T. Beurskens, G. Admiraal, G. Beurskens, W. P. Bosman, S. Garcia-Granda, R. O. Gould, J. M. M. Smits, C. Smykalla, *PATTY, The DIRDIF Program System;* Technical Report of the Crystallography Laboratory, University of Nijmegen: Nijmegen, The Netherlands, 1992.

[7] *CrystalStructure 3.8: Crystal Structure Analysis Package;* Rigaku Americas: The Woodlands, TX, 2000.

[8] J. R. Carruthers, J. S. Rollett, P. W. Betteridge, D. Kinna, L. Pearce, A. Larsen, E.

Gabe, *CRYSTALS Issue 11;* Chemical Crystallography Laboratory: Oxford, U.K., 1999.

[9] Gaussian 09, Revision C.01, M. J. Frisch, G. W. Trucks, H. B. Schlegel, G. E. Scuseria, M. A. Robb, J. R. Cheeseman, G. Scalmani, V. Barone, B. Mennucci, G. A. Petersson, H. Nakatsuji, M. Caricato, X. Li, H. P. Hratchian, A. F. Izmaylov, J. Bloino, G. Zheng, J. L. Sonnenberg, M. Hada, M. Ehara, K. Toyota, R. Fukuda, J. Hasegawa, M. Ishida, T. Nakajima, Y. Honda, O. Kitao, H. Nakai, T. Vreven, J. A. Montgomery, Jr., J. E. Peralta, F. Ogliaro, M. Bearpark, J. J. Heyd, E. Brothers, K. N. Kudin, V. N. Staroverov, R. Kobayashi, J. Normand, K. Raghavachari, A. Rendell, J. C. Burant, S. S. Iyengar, J. Tomasi, M. Cossi, N. Rega, J. M. Millam, M. Klene, J. E. Knox, J. B. Cross, V. Bakken, C. Adamo, J. Jaramillo, R. Gomperts, R. E. Stratmann, O. Yazyev, A. J. Austin, R. Cammi, C. Pomelli, J. W. Ochterski, R. L. Martin, K. Morokuma, V. G. Zakrzewski, G. A. Voth, P. Salvador, J. J. Dannenberg, S. Dapprich, A. D. Daniels, Ö. Farkas, J. B. Foresman, J. V. Ortiz, J. Cioslowski and D. J. Fox, Gaussian, Inc., Wallingford CT, 2009.